Protein Dissection of the Antiparallel Coiled Coil from *Escherichia coli* Seryl tRNA Synthetase†

Martha G. Oakley and Peter S. Kim*

Howard Hughes Medical Institute, Whitehead Institute for Biomedical Research, Department of Biology, Massachusetts Institute of Technology, Cambridge, Massachusetts 02142

Received September 20, 1996; Revised Manuscript Received December 23, 1996⊗

ABSTRACT: The α-helices of coiled-coil proteins are predominantly parallel, in contrast to the general preference for an antiparallel orientation of interacting α-helices found in globular proteins. One intriguing exception is the antiparallel, two-stranded coiled coil comprising the long helical arm of the bacterial seryl tRNA synthetases (SRS). A recombinant 82-residue peptide corresponding to the helical arm of *Escherichia coli* SRS folds into a stable, monomeric, helical structure in the absence of the rest of the protein, as shown by circular dichroism (CD) and equilibrium sedimentation centrifugation. However, peptides corresponding to the individual helices of SRS are unstructured at neutral pH and do not associate appreciably at total peptide concentrations up to 100 μM. Covalent attachment of the the two peptides through a nonnatural, disulfide-containing linker restores structure and allows study of variants in which the individual helices are constrained to interact in either an antiparallel or a parallel orientation. We find that the antiparallel species are substantially more helical and more stable to thermal denaturation than their parallel counterpart. Thus, the SRS helical arm is an autonomously folding unit, and, unlike most other coiled coils, has an intrinsic preference for an antiparallel orientation of its constituent helices.

The class of coiled-coil proteins includes fibrous proteins, such as myosin and keratin (Cohen & Parry, 1990), and the bZip class of transcription factors, which contain coiled-coil dimerization domains (Landschulz et al., 1988; O'Shea et al., 1989a, 1991). Coiled coils consist of two or more interacting α-helices that associate in a parallel or antiparallel orientation. The α-helices of naturally occurring coiled coils are generally parallel. This preference for a parallel orientation is not understood, especially as helices in globular proteins prefer an antiparallel orientation (Richardson, 1981). Indeed, it has been proposed that an antiparallel helix orientation should be favored, based on helix-dipole considerations (Hol et al., 1981; Sheridan et al., 1982). Although they are less common than parallel coiled coils, antiparallel coiled coils do exist. The structures of several proteins containing exposed antiparallel, two-stranded coiled coils have been determined, including *Escherichia coli* and *Thermus thermophilus* SRS,[1] *E. coli* GreA, and the *Bacillus subtilis* replication terminator protein (Cusack et al., 1990; Biou et al., 1994; Bussiere et al., 1995; Stebbins et al., 1995).

E. coli SRS is a dimeric, class II aminoacyl-tRNA synthetase, with each monomer containing two structural domains: a globular catalytic domain, conserved among class II enzymes, and an N-terminal coiled-coil domain (Figure 1) (Cusack et al., 1990). Low-resolution X-ray crystallography data demonstrate that the coiled coil contacts the variable arm of $tRNA^{Ser}$ (Price et al., 1993), and higher-resolution data from the homologous *T. thermophilus* enzyme

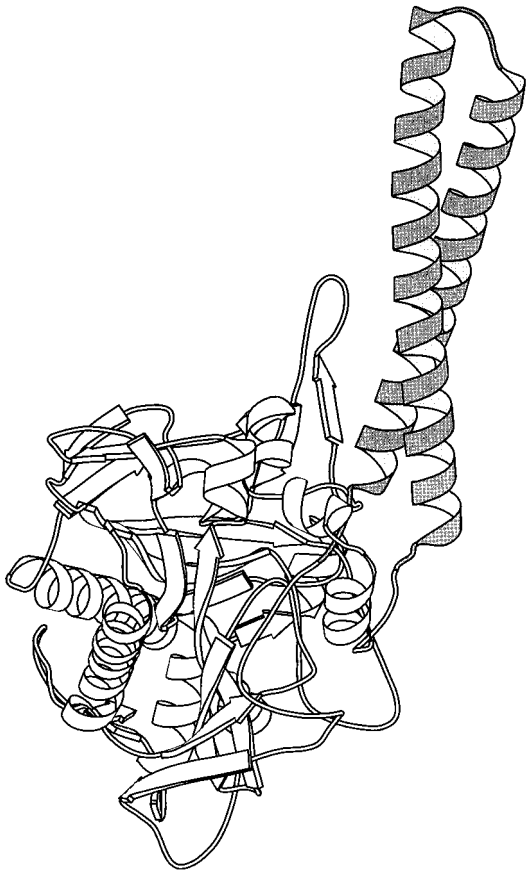

FIGURE 1: A schematic representation of *E. coli* SRS (Cusack et al., 1990). The antiparallel coiled-coil domain (residues 27−100) is indicated by shading. Drawn using the program MOLSCRIPT (Kraulis, 1991) with coordinates provided by Dr. Stephen Cusack.

† Supported by Grant GM44162 from the National Institutes of Health and a Helen Hay Whitney postdoctoral fellowship to M.G.O.

* Author to whom correspondence should be addressed.

⊗ Abstract published in *Advance ACS Abstracts,* February 15, 1997.

[1] Abbreviations: $\Delta G°$, free energy of unfolding; $[\theta]_{222}$, molar ellipticity at 222 nm; k_{ex}, observed amide exchange rate; k_{int}, rate of amide exchange observed in a random polypeptide; CD, circular dichroism; CNBr, cyanogen bromide; GdnHCl, guanidine hydrochloride; HPLC, high-performance liquid chromatography; IPTG, isopropylthio-β-D-galactoside; NMR, nuclear magnetic resonance; PCR, polymerase chain reaction; ppm, parts per million; SRS, seryl tRNA synthetase; T_m, midpoint of the thermal unfolding transition.

S0006-2960(96)02391-4 CCC: $14.00

show extensive interactions between the coiled coil and the variable arm and TΨC loop of the tRNA (Biou et al., 1994). Biochemical data establish the functional importance of this interaction: deletion of the tRNA variable arm or the SRS helical arm leads to a dramatic reduction of aminoacylation activity (Himeno et al., 1990; Normanly et al., 1992; Sampson & Saks, 1993; Borel et al., 1994).

The 60 Å helical arm of SRS consists of two antiparallel α-helices (residues 27−64 and 69−100), denoted H3 and H4, respectively (Cusack et al., 1990). The two SRS helices in the intact protein are fixed relative to each other, by the globular domain at one end, and by a short loop at the other (Figure 1) (Cusack et al., 1990). Because these additional constraints may contribute to the observed antiparallel orientation of the two helices, an inherent preference for an antiparallel helical alignment in the SRS coiled coil cannot be assumed. In the present work, we investigate the influence of these additional constraints on helix orientation preference through a stepwise dissection of the *E. coli* SRS helical arm. We find that the SRS helical arm is an autonomously folding unit. Moreover, we observe that, in contrast to the bZip leucine zipper domains (O'Shea et al., 1989a, 1989b, 1991), the helices of the SRS arm have an intrinsic preference for an antiparallel orientation.

MATERIALS AND METHODS

Plasmid Construction. DNA manipulations were carried out by standard methods (Sambrook et al., 1989). All mutations were made by Kunkel mutagenesis (Kunkel et al., 1987), and each construct was confirmed by DNA sequencing (Sanger et al., 1977). Plasmid pSRS-82, encoding the SRS arm (residues 25−82; Figure 2A), was constructed by PCR amplification from genomic *E. coli* DNA, followed by subcloning into the *Nde*I−*Bam*HI restriction site of the cloning vector pAED4 (Doering, 1992). The oligonucleotide primers 5′-CTGGATGTAGATAAGCTGGGCGCTCT-TGAAGAGCGT-3′ and 5′-AGGGATGGTCAGCGC-GATATCGCGAATTTCAGCCTG-3′ were used for the initial round of PCR amplification. A second round, using the primers 5′-GCGTTAGGCATATGCTGGATGTAG-ATAAGCTGGGCGCTCTTGAA-3′ and 5′-AGTAGAG-GATCCTGACCAAGGGATGGTCAGCGCGAT-ATCGCGAATTTC3′, led to the incorporation of *Nde*I and *Bam*HI restriction sites, as well as a stop codon and codons for an N-terminal Met residue and a C-terminal Trp residue for concentration determination.

Plasmids for the expression of fusion proteins were used to generate the peptides H4, H4-C, H3, and H3-C (Figure 2B) upon cleavage by cyanogen bromide (CNBr). Plasmids pSRS-H4 and pSRS-H4C, constructed for the expression of H4 and H4-C, respectively, (Figure 2B), were derived from pSRS-82 by the introduction of a methionine residue immediately prior to the desired N-terminus to generate a site for cleavage by CNBr. Constructs encoding the H3 and H3-C peptides (Figure 2B) were obtained by the introduction of a Trp codon and a stop codon immediately after the desired C-terminus. The appropriate sequences were inserted to generate the desired cysteine-containing linkers.

The SRS-H3 genes were then subcloned into the *Hin*dIII−*Bam*HI restriction site of the vector pTMHa, kindly provided by Michael Milhollen, to produce plasmids pSRS-H3 and pSRS-H3C. In this kanamycin-resistant vector, the desired sequences are expressed as fusion proteins containing the

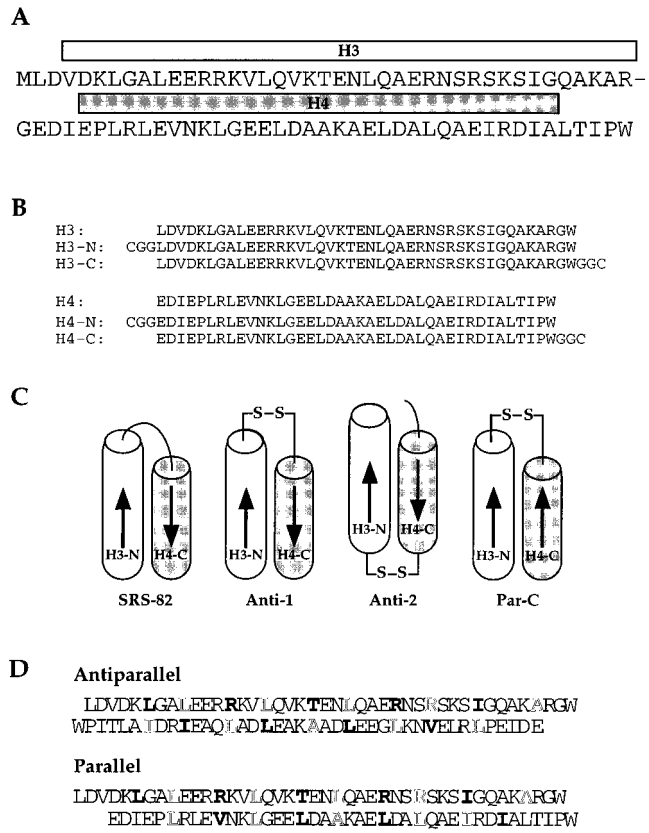

FIGURE 2: (A) Sequence of SRS-82, consisting of SRS residues 25−104, with an additional N-terminal Met residue, as well as a C-terminal Trp for concentration determination. Open and shaded rectangles indicate the constituent helices of the antiparallel coiled coil, H3 and H4, respectively. (B) Sequences of the various SRS peptides. H3 consists of SRS residues 25−65, as well as a C-terminal Trp residue. H4 comprises residues 66−104 of SRS and a C-terminal Trp. H3-N and H3-C contain Cys residues on flexible linkers at the N- and C-terminus, respectively, as do H4-N and H4-C. (C) Schematic representations of the parallel and antiparallel disulfide-containing species with respect to SRS-82. (D) Putative alignments maximizing hydrophobic contacts for the SRS helices in antiparallel and parallel orientations. Residues at the **a** and **d** positions are indicated by bold and outline type, respectively.

Trp ΔLE leader sequence, in which Met residues have been replaced by Leu and Cys residues by Ala (Staley & Kim, 1994), and a sequence of nine His residues has been added at the N-terminus. pTMHa is a derivative of pET-24a (Novagen), in which the modified Trp ΔLE leader sequence, including a *Hin*dIII site after Ala 105 of the leader sequence, has been inserted into the *Nde*I−*Bam*HI site, followed by deletion of the pET-24a *Hin*dIII site and His·Tag sequence.

Protein Expression and Purification. The recombinant proteins SRS-82, H3, H3-C, H4, and H4-C (Figure 2) were expressed in *E. coli* strain BL21 (DE3) pLysS using the T7 system (Studier et al., 1990). Each protein was grown from an overnight culture derived from a single colony with shaking at 37 °C in Luria broth containing 100 μg/mL of ampicillin (SRS-82, H4, and H4-C) or kanamycin (H3 and H3-C) and 25 μg/mL of chloramphenicol. Protein expression was induced at $A_{600} = 0.4-1.0$ by addition of IPTG to 0.4 mM. Cells were harvested after 3−5 h by centrifugation and lysed by freezing and sonication in 50 mM Tris, 25% sucrose, and 1 mM EDTA, pH 8. SRS-82 and the H4 peptides were purified from the soluble fraction by gel filtration (Sephadex, G-75 or G-50). H4 and H4-C peptides

were generated by cleavage with CNBr (0.01−0.05 g/mL, 70% formic acid, 1 h) (Gross, 1967). Cys-containing proteins were protected as homodimers or glutathione-mixed disulfides prior to CNBr treatment. The homodimers were formed by air oxidation (O'Shea et al., 1993); mixed disulfides were generated in the presence of a large (>10-fold) excess of oxidized glutathione (Sigma). Protected peptides were purified by reverse-phase HPLC, using a Vydac C_{18} column and a linear water/acetonitrile gradient containing 0.1% trifluoroacetic acid, to remove unreacted peptide and excess glutathione.

The H3 fusion proteins, containing the Trp ΔLE leader sequence, formed inclusion bodies. The insoluble fraction of the cell lysate was washed with lysis buffer and with 20 mM Tris, 1% Triton X-100, and 1 mM EDTA, pH 8. The resulting pellet was solubilized in 6 M GdnHCl, 0.1 M sodium phosphate, and 10 mM Tris, pH 8.7. Cys-containing fusion peptides were incubated overnight in this buffer with excess oxidized glutathione to form mixed disulfides. The solution was passed over a nickel-chelating column (Ni^{2+}−NTA−Agarose, Qiagen). Bound fractions containing the His tag were eluted with a 6 M GdnHCl buffer containing 0.2 M acetic acid. After dialysis and lyophilization, proteins were treated with CNBr as described above. After removal of CNBr under reduced pressure (Savant speedvac), the solution was brought to pH ∼8 with saturated NaOH, and GdnHCl was added to a concentration of ∼6 M. The solution was again passed over a nickel-chelating column to remove the leader sequence containing the His tag and any uncleaved fusion protein.

H3-N and H4-N peptides (Figure 2B) were synthesized by solid-phase methods and purified by HPLC as described previously (O'Shea et al., 1993).

Final purification of all peptides was by reverse-phase HPLC, as described above. The identity of each peptide was confirmed by laser desorption mass spectrometry on a Voyager Elite mass spectrometer (PerSeptive Biosystems). In all cases, the observed and expected molecular masses agreed to within 0.1% of the calculated peptide mass.

Cys-containing peptides were air-oxidized to form disulfide-linked heterodimers (Figure 2C and D) (O'Shea et al., 1991). H3-C and H4-C were allowed to react in 0.2 M Tris, 5 M GdnHCl, pH 8.7, for 12−24 h to form Par-C. Antiparallel species were allowed to react in 0.2 M Tris, pH 8.7, for 12−24 h. H3-C and H4-N were combined to form Anti-1; H3-N and H4-C were combined to form Anti-2. The desired oxidized heterodimeric species were separated from unreacted starting material and oxidized homodimers by reverse-phase HPLC.

CD Spectroscopy. CD spectra were acquired with Aviv 60DS and 62DS spectrometers. Samples were prepared in 10 mM sodium phosphate and 50 mM sodium chloride, pH 7, unless otherwise noted. Peptide concentrations were determined by Trp absorbance in 5−6 M GdnHCl, assuming an extinction coefficient of 5600 M^{-1} cm^{-1} at 281 nm for Trp (Edelhoch, 1967). Helix content was calculated by the method of Chen et al. (1974). The wavelength dependence of $[\theta]$ was monitored at 0 °C by 3−5 scans acquired in 1-nm increments with a sampling time of 10 s. Thermal stability was determined by monitoring the change in $[\theta]_{222}$ as a function of temperature. The temperature was increased in 2° increments with an equilibration time of 90 s and a data collection time of 30 s. All melts were reversible, with superimposable folding and unfolding curves and >90% of the signal regained upon cooling. Stability to urea denaturation was determined by monitoring $[\theta]_{222}$ as a function of deuterated urea concentration at 0 °C in a D_2O buffer, containing 10 mM sodium phosphate and 50 mM sodium chloride, pH 6.0. Data were analyzed by the linear extrapolation method (Pace et al., 1989). pH readings in D_2O were not corrected for the isotope effect.

Table 1: Molecular Weight Determination by Sedimentation Equilibrium Ultracentrifugation (Rotor Speeds and Initial Concentrations for Each Sample Are Listed)

protein	concn (μM)	M_r/M_r (calc)
SRS-82 (33 krpm, 38 krpm)	250	0.99
	100	0.96
	50	0.97
	30	1.09
	10	0.99
	5	0.93
Anti-1 (28 krpm, 33 krpm)	45	1.18
	15	1.10
	5	1.11
Anti-2 (28 krpm, 33 krpm)	45	1.07
	15	1.02
	5	1.04
Par-C (33 krpm, 38 krpm)	45	1.37[a]
	15	1.13[a]
	5	1.04[a]

[a] Nonrandom residuals in a plot of ln(absorbance) versus radial distance squared, fit assuming a model for a single ideal species, indicating that higher-order association was occurring.

Sedimentation Equilibrium. Apparent molecular masses were determined by sedimentation equilibrium with a Beckman XL-A ultracentrifuge at 4 °C. Samples were dialyzed against 10 mM sodium phosphate, 50 mM sodium chloride, pH 7, for at least 6 h. Concentrations and rotor speeds for each sample are listed in Table 1. Data obtained from two or three wavelengths at two different rotor speeds were fit to a single species model of ln(absorbance) versus radial distance squared using the program NONLIN (courtesy of L. Johnson and J. Lary). Nonrandom residuals, indicative of aggregation or deviations from ideality were observed only for Par-C. Partial molar volumes and solvent densities were calculated as described by Laue et al. (1992).

NMR Spectroscopy. NMR spectroscopy was performed with a Bruker AMX spectrometer operating at 500.1 MHz for ^1H. Samples were approximately 1 mM in 10 mM sodium phosphate, 50 mM sodium chloride, pH 6, and referenced internally to 0 ppm with trimethylsilylpropionic acid. One-dimensional data sets were acquired at 0 °C using a spectral width of 6024.1 Hz and solvent presaturation. Data sets were defined by 4096 complex points and zero-filled once before Fourier transformation. Hydrogen exchange studies were initiated by solvent exchange of a water sample over a spin column (Sephadex G-25) pre-equilibrated with deuterated buffer for at least 12 h [cf. Davidson et al. (1995)]. The sample was diluted by a factor of ca. 2 during this procedure. An average intrinsic amide exchange rate (k_{int}) of 11 min^{-1} was used, corresponding to three times the rate of amide exchange for poly-DL-alanine at pH 6 and 0 °C (Englander et al., 1972). Although the most highly protected amide resonances were not well resolved, an overall exchange rate constant (k_{ex}), was estimated by an analysis of peak intensities over 23 time points (2048 scans each) between 8 and 57 h.

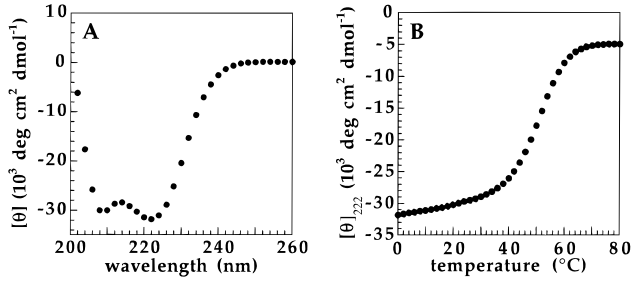

FIGURE 3: (A) Circular dichroism (CD) spectrum of SRS-82 (0 °C, 100 μM, pH 7). The minima near 208 and 222 nm indicate that the peptide is helical. The value for $[\theta]_{222}$ of −31,000 indicates that SRS-82 is ca. 85% helical under these conditions (expected from the crystal structure: 85%). (B) Temperature dependence of the CD signal at 222 nm for SRS-82 (100 μM, pH 7). The T_m of the thermal unfolding transition is ∼50 °C.

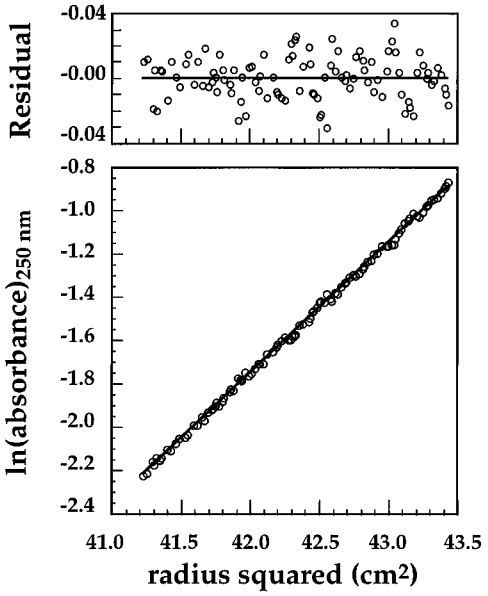

FIGURE 4: Representative analytical ultracentrifugation sedimentation data for SRS-82 at a single wavelength (4 °C, 100 μM, pH 7.0). Data were collected at two or three wavelengths for initial peptide concentrations ranging from 5 to 250 μM (Table 1). The random distribution of the residuals indicates that the data fit well to an ideal single-species model.

RESULTS AND DISCUSSION

SRS Helical Arm. CD spectra demonstrate that the recombinant 82-residue protein SRS-82 is helical at neutral pH and exhibits a cooperative, thermally-induced unfolding transition (Figure 3). The magnitude of $[\theta]_{222}$ coincides with that expected from the structure of intact SRS (Figure 3A), suggesting that this peptide is fully folded in a native conformation. In addition, sedimentation equilibrium experiments demonstrate that SRS-82 is a monomer in solution over a concentration range of 5−250 μM (Figure 4; Table 1). We conclude from these data that the two helices in the SRS arm associate to form a monomeric hairpin structure.

The structural uniqueness of SRS-82 was probed by proton-deuterium amide hydrogen exchange. In contrast to many designed proteins, naturally occurring globular proteins typically contain a subset of amide protons with hydrogen exchange rates approximately an order of magnitude slower than expected if exchange occurred only from globally unfolded molecules [see discussion in Lumb and Kim (1995)]. A small subset of amide protons in SRS-82 is strongly protected from amide exchange (Figure 5B). The most protected amide protons exchange over 10-fold more

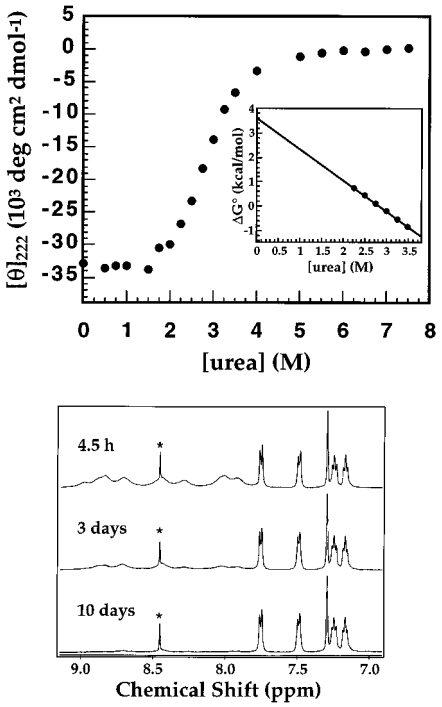

FIGURE 5: (A) Urea denaturation curve for SRS-82 (0 °C, 10 μM, pH 6, D_2O). The data were fit for unfolding of a monomer to yield an apparent $\Delta G°$ of −3.6 kcal/mol (inset). (B) ^1H amide hydrogen exchange studies of SRS-82 (0 °C, pH 6.0, ca. 0.5 mM protein). To collect the data 16 384 scans were used. The resonance marked by an asterisk arises from an impurity. The predicted protection factor, k_{ex}/k_{int}, expected from the global stability of the molecule, is 10^3; the observed protection factor for the most slowly exchanging amides is even greater (10^4−10^5), suggesting that these amides exchange through a global unfolding mechanism. These results provide strong evidence that SRS-82 has a well-packed interior.

slowly than expected from the global stability of the peptide, as determined by urea denaturation in D_2O (Figure 5A), indicating a well-packed helical interface.

These data demonstrate that the SRS helical arm forms a stable, monomeric structure in the absence of the SRS globular domain. The extent of α-helicity, the cooperative nature of the thermal and denaturant-induced melting transitions, and the slow amide hydrogen exchange rates observed for the SRS arm provide strong evidence that the SRS arm folds into a well-packed structure very similar to the α-helical hairpin found in the intact SRS protein. The SRS arm therefore contains the sequence information necessary to adopt its native structure and can be considered an autonomously folding unit (Wetlaufer, 1973).

Helix Orientation. The isolated peptides H3 and H4, which together contain all the residues found in the SRS arm (Figure 2), are largely unstructured at neutral pH. This lack of structure for the constituent helices of a heterodimeric coiled coil has been observed previously for the isolated peptides of "Peptide Velcro", a designed heterodimeric coiled coil (O'Shea et al., 1993). Unlike Peptide Velcro, however, no change in structure was observed by CD upon mixing the H3 and H4 peptides (100 μM total peptide concentration), indicating that these peptides do not associate under these conditions.

To determine whether structure can be restored through a nonnatural linker, H3 and H4 peptides were synthesized with Cys-Gly-Gly- or Gly-Gly-Cys-containing linkers at the N- or C-terminus, respectively (Figure 2B). Covalently-linked heterodimers (Figure 2C and D), constrained to interact in

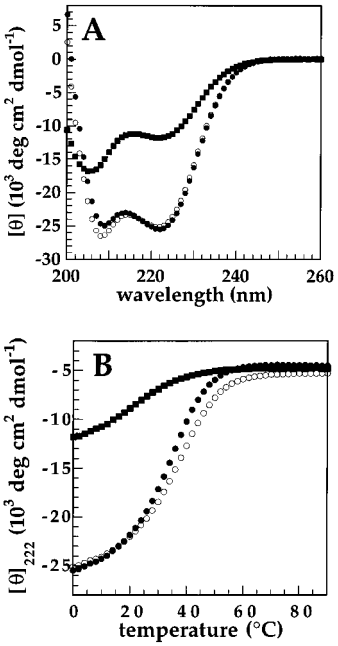

FIGURE 6: (A) CD spectra (0 °C, 10 μM peptide, pH 7) for Par-C (closed squares), Anti-1 (closed circles), and Anti-2 (open circles). The value for $[\theta]_{222}$ of ca. −25 000 indicates that the antiparallel species are approximately 70% helical (calcd 80%). (B) Temperature dependence of the CD signal at 222 nm for the three species described above (10 μM, pH 7). Anti-1 shows a thermal unfolding transition with a T_m of ∼37 °C; Anti-2 a T_m of ∼38 °C. Par-C appears to be partially unfolded at 0 °C.

either a parallel or an antiparallel orientation, were produced through oxidation of the appropriate Cys-containing linkers (O'Shea et al., 1989a). CD studies show that the two antiparallel species, Anti-1 and Anti-2, are helical and exhibit thermally induced unfolding transitions (Figure 6). The antiparallel species have approximately 85% of the helicity expected from a fully folded species (Figure 6A), indicating that structure is largely restored by the nonnatural linker. Sedimentation equilibrium data are consistent with a monomeric state for both species (Table 1), suggesting that the disulfide-linked helices form a hairpin structure.

The two antiparallel species are of comparable helicity (Figure 6A) and stability to thermal denaturation (Figure 6B), demonstrating that a nonnatural linker may be placed at either end of the coiled coil. However, the disulfide-linked species are slightly less helical than the intact SRS arm, possibly due to fraying at the ends of the helices. In addition, the thermal stabilities of both antiparallel disulfide-containing species (Figure 6B) are noticeably reduced, as compared to the SRS arm peptide with its natural linker (Figure 3B). The loop region (residues 65−68) interacts with neighboring residues in the crystal structure of intact SRS (Cusack et al., 1990); some of these interactions may be diminished by the insertion of the linker sequence.

In contrast to the antiparallel species, Par-C, in which the helices are linked in the nonnatural parallel orientation, is considerably less helical and less stable than either antiparallel species (Figure 6). In addition, the apparent molecular weight of Par-C changes with concentration, suggesting formation of higher-order oligomers (Table 1).

Although the constituent helices of the SRS arm fail to associate at reasonable concentrations in an intermolecular fashion, the use of a nonnatural disulfide-containing linker, to form an intramolecular coiled coil, allows an approximate assessment of helix orientation preference. The clear difference in both helix content and stability found between the antiparallel and parallel species suggests that the SRS arm contains sequence features that stabilize an antiparallel coiled coil over a parallel one.

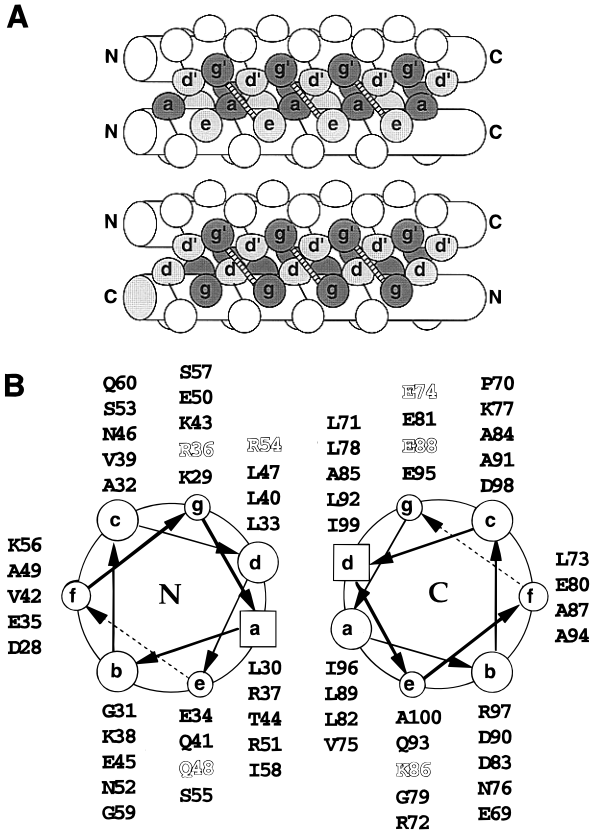

FIGURE 7: (A) Schematic representations of parallel (top) and antiparallel (bottom) coiled-coil structures illustrating the differences in the interactions between the residues at the dimeric interface with respect to helical orientation. Side views of the structures are shown; residues from one helix are labeled **a**−**g**; residues from the other are labeled **a**′−**g**′. Interface residues are indicated: those at the **a**, **a**′, **g**, and **g**′ positions are lightly shaded and those at the **d**, **d**′, **e**, and **e**′ positions are darkly shaded. In the parallel coiled coil, electrostatic interactions can occur between **e** and **g**′, or **g** and **e**′ residues; in the antiparallel coiled coil, **g** residues interact with **g**′ residues and **e** with **e**′. Similarly, **a** residues pack against **a**′ residues and **d** against **d**′ in the parallel coiled coil, but **a** residues pack against **d**′ residues and **d** against **a**′ in the antiparallel case. (B) Helical wheel representation of the SRS coiled coil. Residues 27−60 and 60−100 are shown. Residues involved in hydrogen bonds (R36-E88; Q48-K86; and R54-E74) are indicated by outline type.

The sequences of both parallel and antiparallel coiled coils are characterized by a heptad repeat of seven amino acid residues, denoted **a**−**g** (McLachlan & Stewart, 1975). The residues at positions **a** and **d** are predominantly apolar, forming a 4−3 hydrophobic repeat, with charged residues occurring frequently at **e** and **g** positions (Hodges et al., 1972; McLachlan & Stewart, 1975; Parry, 1982; Lupas et al., 1991; Berger et al., 1995). Residues at these four positions form the hydrophobic interface between α-helices and can participate in interhelical electrostatic interactions (O'Shea et al., 1991; Harbury et al., 1993; 1994; Glover & Harrison, 1995).

Parallel and antiparallel coiled coils differ in several interactions that may give rise to orientation specificity (Figure 7A). Whereas salt bridges can form between **e** and **g**′, or **e**′ and **g** residues in parallel coiled coils (O'Shea et al., 1991; Glover & Harrison, 1995), **e** residues interact with **e**′ residues and **g** residues interact with **g**′ residues in

antiparallel coiled coils (Cusack et al., 1990; Biou et al., 1994; Bussiere et al., 1995; Stebbins et al., 1995). Another difference between parallel and antiparallel coiled coils is the packing at **a** and **d** positions. In parallel structures, **a** residues pack against **a′** residues and **d** residues pack against **d′** residues (O'Shea et al., 1991) but, in antiparallel coiled coils, **a** residues pack against **d′** residues and **d** residues pack against **a′** residues (Cusack et al., 1990; Monera et al., 1993).

Interactions between charged residues at the **e** and **g** positions, between hydrophobic residues at the **a** and **d** positions, and between buried polar residues strongly influence partner specificity or oligomerization state in parallel coiled coils (O'Shea et al., 1992, 1993; Harbury et al., 1993, 1994; Lumb & Kim, 1995; Nautiyal et al., 1995). Such interactions may also play a role in determining orientation preference in coiled coils. For example, the presence of potentially attractive or repulsive interactions at the **e** and **g** positions has been reported to affect orientation preference in model coiled coils (Monera et al., 1993, 1994). Similarly, it has been suggested that the relative positions of large and small hydrophobic residues in the interior of a coiled coil influences helix orientation preference (Gennert et al., 1995; Monera et al., 1996). In addition, there is a buried polar interaction in the SRS helical arm, between R-54 at a **d** position in H3 and E-74 at a **g′** position in H4 (Figure 7B) (Cusack et al., 1990), that may play a role in orientation specificity. The relative importance of surface salt bridges, hydrophobic packing, and buried polar interactions for the observed antiparallel helix orientation in the SRS helical arm remains to be determined.

CONCLUSION

An 82-residue peptide corresponding to the N-terminal domain of *E. coli* seryl tRNA synthetase can assume its two-stranded, antiparallel coiled-coil structure in the absence of the SRS globular domain. This helical hairpin can therefore be considered an autonomously folding unit. Further dissection of this unusual antiparallel coiled coil demonstrates that, in contrast to the parallel coiled coils of the bZip transcription factors, the constituent helices of the SRS coiled coil have an intrinsic preference for an antiparallel helix orientation. Thus, even though the α-helices in known coiled-coil proteins are generally parallel, sequence features within naturally occurring, two-stranded coiled coils can favor either a parallel or an antiparallel relative helix orientation.

ACKNOWLEDGMENT

We thank M. W. Burgess, S. Britt, and J. Pang for peptide synthesis and mass spectrometry; M. A. Millhollen for construction of the plasmid pTMHa; K. J. Lumb and C. J. McKnight for assistance with NMR experiments; and K. J. Lumb, P. B. Harbury and L. C. Wu for many helpful discussions.

REFERENCES

Berger, B., Wilson, D. B., Tonchev, T., Milla, M., & Kim, P. S. (1995) *Proc. Natl. Acad. Sci. U.S.A. 92*, 8259.
Biou, V., Yaremchuk, A., Tukalo, M., & Cusack, S. (1994) *Science 263*, 1404.
Borel, F., Vincent, C., Leberman, R., & Hartlein, M. (1994) *Nucleic Acids Res. 22*, 2963.
Bussiere, D. E., Bastia, D., & White, S. W. (1995) *Cell 80*, 651.
Chen, Y., Yang, J. T., & Chau, K. H. (1974) *Biochemistry 13*, 3350.
Cohen, C., & Parry, D. A. D. (1990) *Proteins 7*, 1.
Crick, F. H. C. (1953) *Acta Crystallogr. 6*, 689.
Cusack, S., Berthet-Colominas, C., Hartlein, M., Nassar, N., & Leberman, R. (1990) *Nature 347*, 249.
Davidson, A. R., Lumb, K. J., & Sauer, R. T. (1995) *Nat. Struct. Biol. 2*, 856.
Doering, D. S. (1992) Ph.D. Thesis, Massachusetts Institute of Technology.
Edelhoch, H. (1967) *Biochemistry 6*, 1948.
Englander, S. W., Downer, N. W., & Teitelbaum, H. (1972) *Annu. Rev. Biochem. 41*, 903.
Gennert, K. M., Surles, M. C., Labean, T. H., Richardson, J. S., & Richardson, D. C. (1995) *Protein Sci. 4*, 2252.
Glover, J. N. M., & Harrison, S. C. (1995) *Nature 373*, 257.
Gross, E. (1967) *Methods Enzymol. 11*, 238.
Harbury, P. B., Zhang, T., Kim, P. S., & Alber, T. (1993) *Science 262*, 1401.
Harbury, P. B., Kim, P. S., & Alber, T. (1994) *Nature 371*, 80.
Himeno, H., Hasegawa, T., Ueda, T., Watanabe, K., & Shimizu, M. (1990) *Nucleic Acids Res. 18*, 446.
Hodges, R. S., Sodek, J., Smillie, L. B., & Jurasek, L. (1972) *Cold Spring Harbor Symp. Quant. Biol. 37*, 299.
Hol, W. G. J., Halie, L. M., & Sander, C. (1981) *Nature 294*, 532.
Kraulis, R. J. (1991) *J. Appl. Crystallogr. 24*, 946.
Kunkel, T. A., Roberts, J. D., & Zakour, R. A. (1987) *Methods Enzymol. 154*, 367.
Landschulz, W. H., Johnson, P. F., & McKnight, S. L. (1988) *Science 240*, 1759.
Laue, T. M., Shah, B. D., Ridgeway, T. M., & Pelletier, S. L. (1992) in *Analytical Ultracentrifugation in Biochemistry and Polymer Science* (Harding, S. E., Rowe, A. J., & Horton, H. C., Eds.) p 90, The Royal Society of Chemistry, Cambridge.
Lumb, K. J., & Kim, P. S. (1995) *Biochemistry 34*, 8642.
Lupas, L., Van Dyke, M., & Stock, J. (1991) *Science 252*, 1162.
McLachlan, A. D., & Stewart, M. (1975) *J. Mol. Biol. 98*, 293.
Monera, O. D., Zhou, N. E., Kay, C. M., & Hodges, R. S. (1993) *J. Biol. Chem. 268*, 19 218.
Monera, O. D., Kay, C. M., & Hodges, R. S. (1994) *Biochemistry 33*, 3862.
Monera, O. D., Zhou, N. E., Lavigne, P., Kay, C. M., & Hodges, R. S. (1996) *J. Biol. Chem. 271*, 3995.
Nautiyal, S., Woolfson, D. N., King, D. S., & Alber, T. (1995) *Biochemistry 34*, 11645.
Normanly, J., Ollick, T., & Abelson, J. (1992) *Proc. Natl. Acad. Sci. U.S.A. 89*, 5680.
O'Shea, E. K., Rutkowski, R., & Kim, P. S. (1989a) *Science 243*, 538.
O'Shea, E. K., Rutkowski, R., Stafford, W. F., & Kim, P. S. (1989b) *Science 245*, 646.
O'Shea, E. K., Klemm, J. D., Kim, P. S., & Alber, T. A. (1991) *Science 254*, 539.
O'Shea, E. K., Rutkowski, R., & Kim, P. S. (1992) *Cell 66*, 699.
O'Shea, E. K., Lumb, K. J., & Kim, P. S. (1993) *Curr. Biol. 3*, 658.
Pace, C. N., Shirley, B. A., & Thomson, J. A. (1989) in *Protein Structure* (Creighton, T. E., Ed.) p 311, IRL Press, Oxford.
Parry, D. A. D. (1982) *Biosci. Rep. 2*, 1017.
Price, S., Cusack, S., Borel, F., Berthet-Colominas, C., & Leberman, R. (1993) *FEBS Lett. 324*, 167.
Richardson, J. S. (1981) *Adv. Protein Chem. 34*, 167.
Sambrook, J., Fritsch, E. F., & Maniatis, T. (1989) in *Molecular Cloning: A Laboratory Manual*, 2nd ed., Cold Spring Harbor Press, Plainview, NY.
Sampson, J. R., & Saks, M. E. (1993) *Nucleic Acids Res 21*, 4467.
Sanger, F., S., N., & Coulson, A. R. (1977) *Proc. Natl. Acad. Sci. U.S.A. 74*, 5463.
Sheridan, R. P., Levy, R. M., & Salemme, F. R. (1982) *Proc. Natl. Acad. Sci. U.S.A. 79*, 4545.
Staley, J. P., & Kim, P. S. (1994) *Protein Sci. 3*, 1822.
Stebbins, C. E., Borukhov, S., Orlova, M., Polyakov, A., Goldfarb, A., & Darst, S. A. (1995) *Nature 373*, 636.
Studier, F. W., Rosenberg, A. H., Dunn, J. J., & Dubendorff, J. W. (1990) *Methods Enzymol. 185*, 60.
Wetlaufer, D. B. (1973) *Proc. Natl. Acad. Sci. U.S.A. 70*, 697.

BI962391T